Appendix A

Review of the Christoffel Equation

This chapter is intended to help fill in some of the background material in basic elasticity theory assumed elsewhere in the thesis.

A.1 Review of notation

The elastic wave equation for a given elastic medium is normally derived by considering the forces acting on an arbitrarily small homogeneous cube of the medium. The variables of interest are **U**, **S**, **T**, and $\underset{\sim}{\mathbf{C}}$.

U is called the particle displacement field. It gives the particle displacement as a function of position. It is not a good measure of strain because it is nonzero for both translations and rotations, neither of which deform the material at all and so should not be associated with strain. So instead of using **U** to measure strain the quantity

$$S_{ij}(\mathbf{r}) = \frac{1}{2}\left(\frac{\partial u_i}{\partial x_j} + \frac{\partial u_j}{\partial x_i}\right) \tag{A.1}$$

is used. The derivatives eliminate the effects of translations, while summing the two "symmetric" terms eliminates the effects of small rotations. Since we are only dealing with tiny deformations anyway, this is no restriction. S_{ij} is called the *strain matrix*. **U** is measured in distance units, whereas **S** is dimensionless. Note that **S** is always symmetric.

Now consider a unit cube. T_{ij} represents a force in the $+i$ direction on the area element

facing the $+j$ direction. This is the *stress matrix*. It is measured in units of force per area. The anti-symmetric part of $\mathbf{T}$ is associated with torque. However, particle rotation plays no part in linear wave propagation. In the absence of external torque, the matrix $\mathbf{T}$ can thus be assumed symmetric.

The strain resulting from a given stress is a property of the medium involved. For small strains, the strain can be assumed to be a linear function of the stress. Since the strain matrix $\mathbf{S}$ and the stress matrix $\mathbf{T}$ are 3×3 matrices, they must be related by a 3×3×3×3 tensor. The elements of the tensor $\underset{\sim}{\mathbf{C}}$ are called *elastic stiffness constants*. Analytically,

$$T_{ij} = \mathrm{C}_{ijkl} S_{kl}. \tag{A.2}$$

The stiffness matrix $\underset{\sim}{\mathbf{C}}$ is measured in the same units as stress. The symmetries of $\mathbf{T}$ and $\mathbf{S}$ require that $\mathrm{C}_{ijkl} = \mathrm{C}_{jikl} = \mathrm{C}_{ijlk}$.

A.1.1 Abbreviated subscripts

Fourth order tensors are inconvenient to write down on paper. Usually $\mathbf{T}$, $\mathbf{S}$, and $\underset{\sim}{\mathbf{C}}$ are not expressed with their natural subscripts but a compact notation is used instead. Symmetry allows each set of two subscripts to be replaced by one, with no attention to the order of the two subscripts: $xx \Longrightarrow 1$, $yy \Longrightarrow 2$, $zz \Longrightarrow 3$, $yz, zy \Longrightarrow 4$, $xz, zx \Longrightarrow 5$, and $xy, yx \Longrightarrow 6$. Thus an expression like C_{24} means C_{yyyz}, which we have already demonstrated is the same as C_{yyzy}. For some of the strain components there are multplicative factors of 2 as well. This transformation reduces $\mathbf{T}$ and $\mathbf{S}$ to 3-vectors, and $\underset{\sim}{\mathbf{C}}$ to a 6×6 matrix. The penalty for this conciseness is a loss of elegance in the equations involved.

A.1.2 Strain energy

Assuming a perfectly elastic material, all of the energy put in while deforming it can be recovered by allowing the material to return to its equilibrium position. The energy expended in straining the material can be calculated in exactly the same way that the energy expended in stretching an ideal spring can. For a spring, the work expended is the integral of force over distance. For a general elastic material the corresponding quantity is the integral of the stress dotted with the differential strain. Mathematically, if $u_{\mathbf{S}_0}$ is

the *strain energy density* associated with the strain $\mathbf{S}_0$, then

$$u_{\mathbf{S}_0} = \int_{\mathbf{0}}^{\mathbf{S}_0} d\mathbf{S}^T \cdot \mathbf{T}. \tag{A.3}$$

Using the relation $\mathbf{T} = \underset{\sim}{\mathbf{C}} \cdot \mathbf{S}$, this can be rewritten as

$$u_{\mathbf{S}_0} = \int_{\mathbf{0}}^{\mathbf{S}_0} d\mathbf{S}^T \cdot \underset{\sim}{\mathbf{C}} \cdot \mathbf{S}. \tag{A.4}$$

As a test we will perform the integral in equation (A.4) along a path that goes directly from $\mathbf{0}$ to $\mathbf{A}$ and then directly from there to $\mathbf{S}_0 = \mathbf{A} + \mathbf{B}$. For the part from $\mathbf{0}$ to $\mathbf{A}$ we get:

$$\int_{\mathbf{0}}^{\mathbf{A}} d\mathbf{S}^T \cdot \underset{\sim}{\mathbf{C}} \cdot \mathbf{S} = \int_0^1 \mathbf{A}^T \cdot \underset{\sim}{\mathbf{C}} \cdot \mathbf{A}\, t\, dt = \frac{1}{2}\, \mathbf{A}^T \cdot \underset{\sim}{\mathbf{C}} \cdot \mathbf{A},$$

and for the part from $\mathbf{A}$ to $\mathbf{A} + \mathbf{B}$ we get:

$$\int_{\mathbf{A}}^{\mathbf{A}+\mathbf{B}} d\mathbf{S}^T \cdot \underset{\sim}{\mathbf{C}} \cdot \mathbf{S} = \int_0^1 \mathbf{B}^T \cdot \underset{\sim}{\mathbf{C}} \cdot (\mathbf{A} + \mathbf{B}t)\, dt = \frac{1}{2}\, \mathbf{B}^T \cdot \underset{\sim}{\mathbf{C}} \cdot \mathbf{B} + \mathbf{B}^T \cdot \underset{\sim}{\mathbf{C}} \cdot \mathbf{A},$$

for a combined integral over the entire path of

$$\frac{1}{2}\, (\mathbf{A}^T \cdot \underset{\sim}{\mathbf{C}} \cdot \mathbf{A} + \mathbf{B}^T \cdot \underset{\sim}{\mathbf{C}} \cdot \mathbf{B}) + \mathbf{B}^T \cdot \underset{\sim}{\mathbf{C}} \cdot \mathbf{A}. \tag{A.5}$$

Instead of the path chosen we might just as well have gone from $\mathbf{0}$ to $\mathbf{B}$ to $\mathbf{S}_0 = \mathbf{B} + \mathbf{A}$ instead. In that case we would have gotten

$$\frac{1}{2}\, (\mathbf{A}^T \cdot \underset{\sim}{\mathbf{C}} \cdot \mathbf{A} + \mathbf{B}^T \cdot \underset{\sim}{\mathbf{C}} \cdot \mathbf{B}) + \mathbf{A}^T \cdot \underset{\sim}{\mathbf{C}} \cdot \mathbf{B}. \tag{A.6}$$

The integral in equation (A.4) cannot depend on which of the two alternate paths we chose, for if it did we could go from the equilibrium position to $\mathbf{S}_0$ by one path and back again to equilibrium by the other, and either create or destroy energy depending on which way we went! So the quantities in equations (A.5) and (A.6) must be equal for all $\mathbf{A}$

and **B**. By identity

$$\mathbf{A}^T \cdot \underset{\sim}{\mathbf{C}} \cdot \mathbf{B} = \mathbf{B}^T \cdot \underset{\sim}{\mathbf{C}}^T \cdot \mathbf{A} \tag{A.7}$$

(the transpose of a scalar is itself); for equations (A.5 and (A.6) to always be equal, is must be that

$$\underset{\sim}{\mathbf{C}} = \underset{\sim}{\mathbf{C}}^T. \tag{A.8}$$

We have found yet another symmetry property of the stiffness matrix.

Given this symmetry, the strain energy density associated with a particular strain $\mathbf{S}_0$ is

$$E = \frac{1}{2}\, \mathbf{S}_0^T \cdot \underset{\sim}{\mathbf{C}} \cdot \mathbf{S}_0, \tag{A.9}$$

regardless of how the material reached that strain state.

In the most general case the stiffness matrix possesses no more symmetries than those already listed here, and the $\underset{\sim}{\mathbf{C}}$ matrix has the form

$$\begin{bmatrix} C_{11} & C_{12} & C_{13} & C_{14} & C_{15} & C_{16} \\ C_{12} & C_{22} & C_{23} & C_{24} & C_{25} & C_{26} \\ C_{13} & C_{23} & C_{33} & C_{34} & C_{35} & C_{36} \\ C_{14} & C_{24} & C_{34} & C_{44} & C_{45} & C_{46} \\ C_{15} & C_{25} & C_{35} & C_{45} & C_{55} & C_{56} \\ C_{16} & C_{26} & C_{36} & C_{46} & C_{56} & C_{66} \end{bmatrix}. \tag{A.10}$$

This leaves only $6 + 5 + 4 + 3 + 2 + 1 = 21$ independent elastic constants out of the original 81.

A.1.3 Symmetry classes

If a medium is symmetric under certain transformations of coordinates, then any mathematical equation representing some property of the medium must also have corresponding symmetries. Thus, for a given crystal symmetry group the stiffness matrix $\underset{\sim}{\mathbf{C}}$ can be simplified to take advantage of the symmetries that are present. The more symmetries there are, the simpler the stiffness matrix for the medium becomes. A complete list of stiffness

matrices for each symmetry group are given in Appendix A.2 of Auld (1973); I will only show the two most important cases here.

For transversely isotropic media (axisymmetric about the z axis), the matrix $\underset{\sim}{\mathbf{C}}$ has only 5 independent constants:

$$\begin{bmatrix} C_{11} & C_{11}-2C_{66} & C_{13} & 0 & 0 & 0 \\ C_{11}-2C_{66} & C_{11} & C_{13} & 0 & 0 & 0 \\ C_{13} & C_{13} & C_{33} & 0 & 0 & 0 \\ 0 & 0 & 0 & C_{55} & 0 & 0 \\ 0 & 0 & 0 & 0 & C_{55} & 0 \\ 0 & 0 & 0 & 0 & 0 & C_{66} \end{bmatrix}. \tag{A.11}$$

For orthorhombic media (symmetry planes corresponding to the axis planes), there are 9 independent constants:

$$\begin{bmatrix} C_{11} & C_{12} & C_{13} & 0 & 0 & 0 \\ C_{12} & C_{22} & C_{23} & 0 & 0 & 0 \\ C_{13} & C_{23} & C_{33} & 0 & 0 & 0 \\ 0 & 0 & 0 & C_{44} & 0 & 0 \\ 0 & 0 & 0 & 0 & C_{55} & 0 \\ 0 & 0 & 0 & 0 & 0 & C_{66} \end{bmatrix}. \tag{A.12}$$

For transversely isotropic or orthorhombic media the axis planes are also symmetry planes, so it makes sense to think of two-dimensional propagation within an axis plane. We accomplish this by discarding a dimension. For example, propagation within the x-z plane will be controlled by the elastic constants involving x and z: $xx \Longrightarrow 1$, $zz \Longrightarrow 3$, and $xz \Longrightarrow 5$, therefore C_{11}, C_{33}, C_{13}, and C_{55}. (The other elastic constants C_{35} and C_{15} are zero because otherwise they would break the symmetry about the other two axis planes. For example, they would become nonzero if the orthorhombic medium were rotated about the y axis.) The effects of the $\{1,3,5\}$ elastic constants within the x-z plane are exactly like the qP-qSV transversely isotropic situation covered in Chapter 2. Namely, C_{11} and C_{55} control the two waves propagating along the x axis, C_{33} and C_{55} control the two waves propagating along the z axis, and C_{13} controls the ellipticity or lack thereof in between. (There are some interesting points here. Note that 3 wavetypes on each of 3 axes would

need 9 elastic constants to specify them, but there are only 6 elastic constants on the diagonal of the $\underset{\sim}{\mathbf{C}}$ matrix. So it's not surprising that C_{55} gets used twice. For the TI case, note that the $C_{11} - 2C_{66}$ term in the $\underset{\sim}{\mathbf{C}}$ matrix is the value of C_{12} for ellipticity in the x-y plane. Since $C_{11} = C_{22}$, the ellipse is in fact a circle, as we already knew it had to be because of the symmetry about the z axis.)

Why did I only mention two wavetypes in the x-z plane? By dropping y we dropped the SH wave in the x-z plane; its particle motion is purely y. We can get the SH wave back by considering the combinations pairing y singly with x and z: $xy \Longrightarrow 6$ and $zy \Longrightarrow 4$, therefore C_{44} and C_{66}. (Again, a nonzero C_{46} would break the symmetry in the other planes.) No more elastic constants are needed to specify the orthorhombic SH wave in the symmetry plane because it is always elliptic.

You may have already noticed the strange ordering of elastic constants in Table C.2. Now you know why: the ordering is just {x-axis, y-axis, z-axis} repeated three times.

A.1.4 Energy constraints

Previously I showed that because of various symmetries there were at most only 21 independent constants in the $\underset{\sim}{\mathbf{C}}$ matrix. Are there any nonsymmetry constraints on the $\underset{\sim}{\mathbf{C}}$ matrix? In equation (A.9 the unperturbed state (no strain) has been assigned a strain energy $E = 0$. This must be an energy minimum, otherwise the medium wouldn't be stable in the unperturbed state; it would spontaneously strain itself, releasing energy in the process! The requirement that the strain energy E be positive for any arbitrary non-zero strain $\mathbf{S}$ is exactly the requirement that the matrix $\underset{\sim}{\mathbf{C}}$ be positive definite.[1] This is the *physical realizability* constraint on $\underset{\sim}{\mathbf{C}}$. In general there are no more constraints beyond those already presented here.

In the isotropic case the energy constraints are

$$\frac{3}{4}C_{11} > C_{55} > 0, \tag{A.13}$$

[1]It is interesting to look at the eigenvalues and eigenvectors of the $\underset{\sim}{\mathbf{C}}$ matrix. The eigenvalues and eigenvectors of the compressed 6×6 form of the matrix seem to lack any clear physical significance, although the signs of the eigenvalues do provide a clear test of physical realizability. Muir (1990) has suggested an alternative $(\{xyz\}\times\{xyz\})\times(\{xyz\}\times\{xyz\}) = 9\times9$ form of the $\underset{\sim}{\mathbf{C}}$ matrix. Three of the 9 eigenvalues of this matrix are always zero, complicating tests of positive-definiteness. The other 6 and their associated eigenvectors, however, seem to provide useful information about the properties of the medium.

hence the isotropic truth that "P waves are always significantly faster than S waves". For transversely isotropic media the energy constraints are

$$C_{11} > C_{66} > 0, \quad C_{33} > 0, \quad C_{55} > 0, \quad \text{and} \quad C_{13}^2 < C_{33}(C_{11} - C_{66}). \tag{A.14}$$

(The corresponding transversely isotropic statement is "the horizontal qP wave is at least barely faster than the horizontal SH wave", not as catchy.)

A.2 The Christoffel equation

We have examined the stiffness matrix $\underset{\sim}{\mathbf{C}}$ now; how do we go from there to the elastic wave equation? The wave equation can be derived from three fundamental relations. These are the *strain-displacement relation*, relating **S** and **U**, the *equation of motion*, relating **T** and **U**, and the *elastic constitutive equation*, relating **T**, $\underset{\sim}{\mathbf{C}}$, and **S**. The first and third of these have already been given above in equations (A.1) and (A.2), respectively; the second is simply Newton's law. These three equations solved simultaneously form the elastic wave equation.

The Christoffel equation is just the elastic wave equation Fourier transformed over space and time, and specifies the propagation velocity and particle-motion direction for each plane wave component in the Fourier domain. The Christoffel equation has the form of an eigenvector-eigenvalue problem:

$$\underset{\sim}{\mathbf{D}}\,\underset{\sim}{\mathbf{C}}\,\underset{\sim}{\mathbf{D}}^T\,\mathbf{v}_n = -\rho\left(\frac{\omega_n}{k}\right)^2 \mathbf{v}_n \quad ;$$

$$\underset{\sim}{\mathbf{D}} = \frac{1}{k}\begin{bmatrix} k_x & 0 & 0 & 0 & k_z & k_y \\ 0 & k_y & 0 & k_z & 0 & k_x \\ 0 & 0 & k_z & k_y & k_x & 0 \end{bmatrix}. \tag{A.15}$$

In this equation ρ and the 6 by 6 symmetric matrix $\underset{\sim}{\mathbf{C}}$ define the homogeneous medium; ρ gives the density and the stiffness matrix $\underset{\sim}{\mathbf{C}}$ gives the elastic constants. The 3 by 6 derivative matrix $\underset{\sim}{\mathbf{D}}$ defines the plane-wave propagation direction under consideration. $\underset{\sim}{\mathbf{D}}$ is a function of the wavenumber vector (k_x, k_y, k_z). The leading $1/k$ normalizes the wavenumber vector ($k = |(k_x, k_y, k_z)| = \sqrt{k_x^2 + k_y^2 + k_z^2}$). Finally, ω_n and $\mathbf{v}_n$ define the

resulting three wave modes; for each n, $\mathbf{v}_n$ is the particle-motion direction, and (ω_n/k) is the associated phase velocity. The matrix $\underset{\sim}{\mathbf{D}}\,\underset{\sim}{\mathbf{C}}\,\underset{\sim}{\mathbf{D}}^T$ is called the Christoffel matrix. Note that since $\underset{\sim}{\mathbf{C}}$ is symmetric, the Christoffel matrix is symmetric.

For a given ρ, $\underset{\sim}{\mathbf{C}}$, and (k_x, k_y, k_z), equation (A.15) always has exactly three solutions; each solution corresponds to one wavetype (Auld, 1973). (Given this definition, we can then conclude that phase velocity is a single-valued function of phase direction for any one wavetype.) Most importantly, because the Christoffel matrix is symmetric the particle-motion vectors $\mathbf{v}_1$, $\mathbf{v}_2$, and $\mathbf{v}_3$ associated with the three solutions are *mutually orthogonal.* If two of the phase velocities are identical, there is some ambiguity in the associated particle-motion directions; we can and will always choose them to be orthogonal. (In fact there is no reason not to go ahead and normalize them, making a complete *orthonormal* set of particle-motion directions.)

The guaranteed existence of three orthogonal wavetypes is a special case of a famous theorem about the eigenvectors of Hermetian[2] matrices: any Hermetian matrix has a complete set of orthonormal eigenvectors (Strang, 1980). We use this property several times in Chapters 2 and 3.

[2] "Hermetian" is just the complex analogue of "symmetric". All real symmetric matrices are also Hermetian.

Appendix B

From Phase to Group (and back again)

In this chapter I will discuss some of the most important concepts in anisotropy, group and phase velocity.

B.1 Group and phase velocity

Figure B.1 shows an idealized wavefront propagating away from a point source at four evenly spaced times. (We could also imagine hanging some wavelet off this idealized wavefront to make it more physically accurate, in which case the wavefronts shown in the figure could be interpreted as constant phase surfaces – i.e., sets of points at the same stage of the wavelet.) The background medium is assumed to be infinite, homogeneous, and nondispersive, so there is no fundamental "distance unit" to the picture, and the wavefronts at different times are merely scaled versions of the same template. As a result, a given blob of energy riding the wavefront must travel along a direct radial line emanating from the source.

Now imagine an observer at some point in the medium watching the wave go by. If he knows where the source was and when it went off, he can easily find the energy (group) velocity in the source-observer direction by measuring the time the wave energy took to travel the known distance along that line.

What if the observer does not know the position or timing of the source? The observer can still see the wavefront pass by his local domain, noting its direction of travel

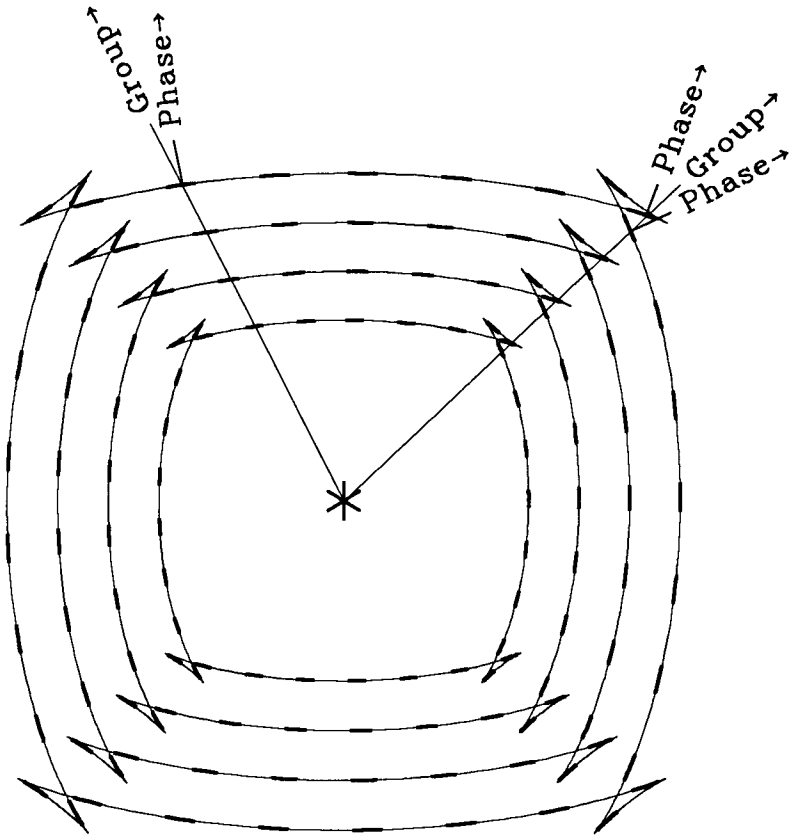

FIG. B.1. A wavefront emanating from a point source in an anisotropic nondispersive medium. The wavefront is shown at four equally spaced times. Hypothetical "blobs of energy" riding on the wavefront are represented by thicker segments on the wavefront curves. The blobs of energy travel straight out from the source (marked by the "*"). The energy propagation direction also defines the group direction. The phase direction is perpendicular to the wavefront surface. Note it is possible for energy to travel with more than one group velocity in a given group direction; the different arrival branches have unique phase directions however. (There are three branches in the example here, even though only two are labelled.)

and velocity. However, the observer can only track an individual phase of the wavefront as it goes by. (You can imagine him sampling the wavefield at several adjacent points and correlating the recorded seismograms to find the time delays between them.) Note in Figure B.1 that the wavefronts themselves are generally *not* perpendicular to the radial lines from the source. Our hypothetical observer cannot detect the energy slipping sideways tangent to the wavefront. The measured *phase* direction and velocity (measured by tracking the wavefront as it passes through some small region of space) will not be the same as the energy (*group*) direction and velocity (measured by stopwatch over the known distance from source to observer).

Phase and group velocity are general concepts, applicable to all kinds of waves in all kinds of homogeneous media, both anisotropic (direction matters) and dispersive (frequency matters). In the remainder of this chapter I will narrow the discussion of phase velocity to the special case of plane waves. Phase velocity as a function of phase direction, frequency, and wavetype is ultimately a fundamental property of the underlying anisotropic medium, not just of plane waves. However, plane waves are particularly useful to think in terms of because they greatly simplify the mathematics; they also form the kernel of Fourier transformation.

In terms of plane waves, then, the *phase velocity* associated with a given direction is the velocity of a plane wave traveling in that direction. The *group velocity* associated with a given direction is the velocity of a blob of energy traveling in that direction.

B.1.1 Why phase and group

Phase velocities are easier to calculate and more tractable mathematically (see section A.2), but since infinite uniform plane waves are rare in the real world group velocity is the more useful quantity. The canonical problem, then, is how to go from the phase velocities provided by the Christoffel equation to the group velocities required for interpreting synthetic or possibly even real data. In this Appendix I will limit my discussion to the two-dimensional version of this problem.

Let V_r (r for ray) be the group velocity; in two dimensions it is a function of the group propagation angle ϕ_r. The polar graph of V_r versus ϕ_r, the *group-velocity curve*[1], is easy to picture physically: it is a snapshot of the wavefront created by the explosion of an ideal

[1]This is also called the *ray surface* in many fields. To emphasize the connection with impulse responses, I will usually call it the "impulse-response surface" elsewhere in the thesis.

point source. (You have already seen an example of such a plot in Figure B.1.) Similarly, let V_w (w for wave) be the phase velocity; in two dimensions it is a function of the plane-wave propagation angle ϕ_w. The polar graph of V_w versus ϕ_w is the *phase-velocity curve*. Phase-velocity curves seem to have no simple physical analogue.

B.1.2 Group to phase

The previous paragraph suggests a simple way to derive $V_w(\phi_w)$ given $V_r(\phi_r)$. A point source is mathematically equivalent to a plane-wave source that radiates plane waves equally in all directions. On a small enough scale any piece of a wavefront (except at a caustic) is indistinguishable from a plane wave. Since the group-velocity curve represents the wavefront created by a point source, the tangent line to the group-velocity curve at any point represents a single plane-wave component radiated by the point source. We can find the velocity of such a plane-wave component by measuring the distance it has traveled. The direction of travel of any plane wave is always given by the wavefront normal. (Uniform plane waves can't slip "sideways" as they travel, because motion in that direction is by definition imperceptible.) Thus, for each V_r and ϕ_r we can construct a corresponding V_w and ϕ_w. (This process can be viewed mathematically as integrating a point Green's function to obtain a line Green's function.)

The process is shown geometrically in Figure B.2. The light solid curve represents the group velocity (V_r), and the light dotted curve the phase velocity (V_w). For each of three points on the group velocity curve, a dark tangent line has been drawn. A second dark line has been drawn from the point source to each tangent line so as to meet it at a right angle. The direction of the second line gives the direction of propagation of the plane wave represented by the tangent. Since the point of intersection of the two lines is also the point on the tangent line that is closest to the point source, the length of the second line is proportional to the phase velocity of the plane wave. Thus the locus of such intersections sweeps out the phase-velocity curve.

It is a simple exercise in trigonometry to find a mathematical formula for V_w and ϕ_w

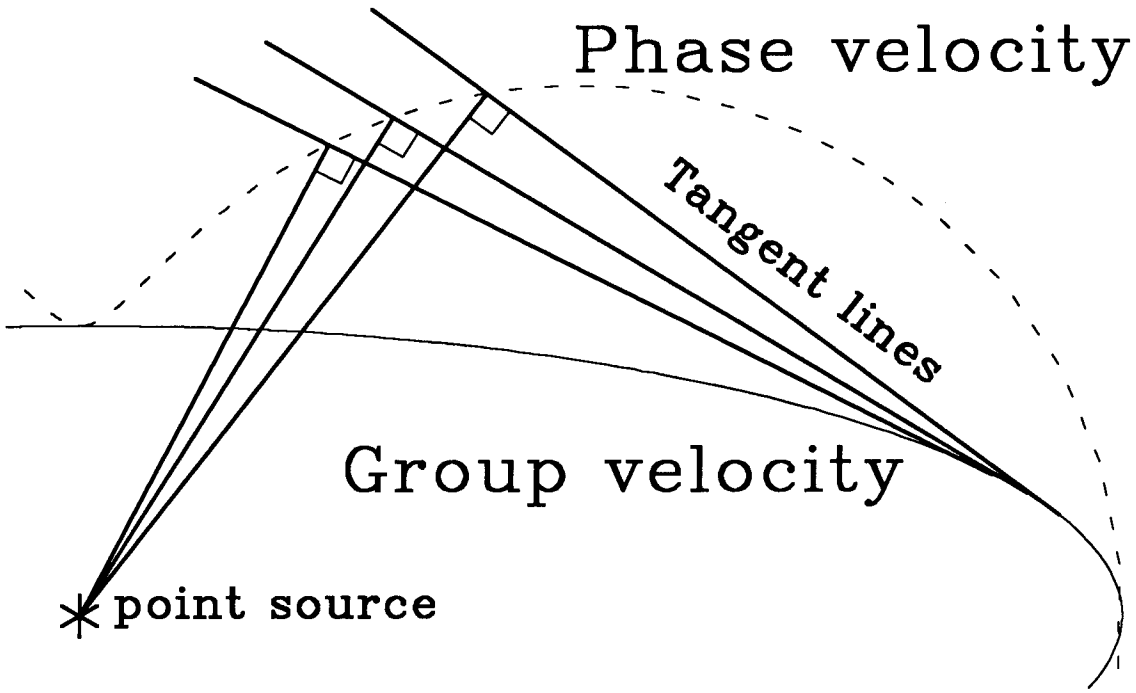

FIG. B.2. A diagram showing the geometrical relationship between the group-velocity curve (solid) and the phase-velocity curve (dotted). In this example the group-velocity curve is an ellipse.

in terms of V_r and ϕ_r using the construction shown in Figure B.2. The result is:

$$V_w = \frac{{V_r}^2}{\sqrt{{V_r}^2 + \left(\frac{dV_r}{d\phi_r}\right)^2}} \quad \text{and} \quad \phi_w = \phi_r - \text{Arctan}\left(\frac{dV_r/d\phi_r}{V_r}\right). \tag{B.1}$$

We will call this transformation "R", since it is closely related to the Radon transform.

B.1.3 Phase to group

Equation B.1 is not very useful. We usually need to go the other direction, from phase velocity to group velocity. It is not obvious how to invert equation (B.1), though. It is most easily done by returning to the physical analogy used to derive equation (B.1).

The phase-velocity curve gives the velocities of plane waves as a function of their direction of travel. Let us examine a pair of plane waves traveling in very nearly the same

direction. The plane waves, being infinite non-parallel lines, must cross somewhere. The point where the waves cross is the point of highest amplitude. If more waves are used, instead of a point there will be a region in which the waves add constructively. Outside of this region the waves will add in a more or less random manner and mostly cancel. Summing a group of plane waves traveling in a narrow range of directions thus results in a moving blob of energy. The velocity of this blob is the group velocity.

We can now return to Figure B.2 and examine it in the terms of the preceding paragraph. In the figure we are summing three plane waves, using the phase-velocity curve to position each one at the correct distance from the source. The curve along which they are summing constructively must be tangent to each plane wave and also pass through the region where they intersect. The group-velocity curve shown satisfies these requirements. In the limit as infinitely close plane waves are used, each point on the phase-velocity curve can be identified with a unique point on the group-velocity curve. As before, the position of this point gives V_r and ϕ_r.

It is an elementary exercise in calculus and trigonometry to find V_r and ϕ_r in terms of V_w and ϕ_w using this construction. The result is:

$$V_r = \sqrt{{V_w}^2 + \left(\frac{dV_w}{d\phi_w}\right)^2} \quad \text{and} \quad \phi_r = \phi_w + \text{Arctan}\left(\frac{dV_w/d\phi_w}{V_w}\right). \tag{B.2}$$

We will call this transformation "R inverse".[2]

The preceding geometrical constructions have a long history, dating back at least to McGullagh (1837). Other notable presentations can be found in Postma (1955), Garmany (1989), and Helbig (1990).

B.1.4 Dispersion relations and phase velocity

In Appendix A I derive the Christoffel equation. The Christoffel equation is just the elastic wave equation Fourier transformed over space and time. It is useful because it reduces the original differential equation into a tractable algebraic one. The solutions are polynomials involving ω, k_x (and k_y in three dimensions) and k_z.

[2]Note in this equation that the group velocity is always greater than or equal to the associated phase velocity. This makes sense if you realize the group velocity must be the vector sum of the phase velocity V_w (perpendicular to the wavefront) *and* the "sideslip" velocity $dV_w/d\phi_w$ (parallel to the wavefront).

Such an equation relating ω, k_x, and k_z is called a *dispersion relation.* A dispersion relation is the Fourier transform of a scalar wave equation. For a vector wave equation, there will be a different dispersion relation for each distinct mode of wave propagation. Dispersion relations are useful because they can be solved for k_z and used to downward and upward continue wavefields.

Dispersion relations are traditionally displayed as a graph of k_z/ω versus k_x/ω for fixed ω.[3] The spatial frequency k of a wave is $k = \sqrt{k_x^2 + k_z^2}$, and the tangent of the direction of propagation is k_x/k_z, so in polar coordinates the dispersion relation is a graph of k/ω as a function of direction. From basic Fourier transform theory, $V_w = \omega/k$. Let us call the inverse of velocity *slowness*, and let us represent it by an upside-down V: $\Lambda_w = k/\omega$. Then a dispersion relation graph is just a plot of *phase slowness* versus phase direction ($\Lambda_w(\phi_w)$) for a particular temporal frequency. Figure B.3 shows a dispersion relation calculated by brute-force Fourier transformation of a two-dimensional finite-difference wavefield. (Note the Fourier-transformation itself is three dimensional, since besides transforming the two space dimensions it also transforms time to frequency.) Another example of a dispersion relation calculated by brute-force Fourier transformation can be found in McMechan and Yedlin (1981).

B.2 Interesting symmetries

In the previous section we found that slowness might be a more natural unit than velocity for some things. This suggests it might be worthwhile to recast equations (B.1) and (B.2) in terms of slowness. A little algebra produces the beautifully symmetric equations shown in Table B.1: the geometrical construction mapping group-velocity curve to phase velocity also maps phase slowness to group slowness! Engineers call such curves "polar reciprocals". For a graphical example of these symmetries, see Figure B.4.

These symmetries can be very useful. For example, we know the phase direction (ϕ_w) is perpendicular to the group-velocity curve $V_r(\phi_r)$. From the symmetry, we now also know the group direction (ϕ_r) is similarly perpendicular to the phase-slowness curve $\Lambda_w(\phi_w)$. (These relations are well known; for a completely different derivation see section 4.2 of Claerbout (1985). He treats the subject while investigating the accuracy of the 15° wave equation. One-way wave equations are, of course, anisotropic by their very nature.)

[3] Dispersion relations are traditionally defined and displayed this way *in Geophysics*, at least. In other fields they are typically displayed as graphs of ω versus a one-dimensional k.

$$V_w = \frac{{V_r}^2}{\sqrt{{V_r}^2 + \left(\frac{dV_r}{d\phi_r}\right)^2}} \quad , \quad \phi_w = \phi_r - \text{Arctan}\left(\frac{dV_r/d\phi_r}{V_r}\right) \qquad \text{(R)}$$

$$\Lambda_r = \frac{\Lambda_w^2}{\sqrt{\Lambda_w^2 + \left(\frac{d\Lambda_w}{d\phi_w}\right)^2}} \quad , \quad \phi_r = \phi_w - \text{Arctan}\left(\frac{d\Lambda_w/d\phi_w}{\Lambda_w}\right) \qquad \text{(R)}$$

$$V_r = \sqrt{{V_w}^2 + \left(\frac{dV_w}{d\phi_w}\right)^2} \quad , \quad \phi_r = \phi_w + \text{Arctan}\left(\frac{dV_w/d\phi_w}{V_w}\right) \qquad \text{(R inverse)}$$

$$\Lambda_w = \sqrt{\Lambda_r^2 + \left(\frac{d\Lambda_r}{d\phi_r}\right)^2} \quad , \quad \phi_w = \phi_r + \text{Arctan}\left(\frac{d\Lambda_r/d\phi_r}{\Lambda_r}\right) \qquad \text{(R inverse)}$$

$$V_r = 1/\Lambda_r \quad , \quad \Lambda_r = 1/V_r \qquad \text{(1/r)}$$

$$V_w = 1/\Lambda_w \quad , \quad \Lambda_w = 1/V_w \qquad \text{(1/r)}$$

Table B.1. Equations relating the group and phase domains, in terms of both velocity V and slowness Λ. There are two transformations involved: "R" (for Radon) and "1/r" (replace the radius r with its reciprocal). (Note "R" and "R inverse" here are also equations (B.1) and (B.2) respectively in the text.) Now examine Figure B.4.

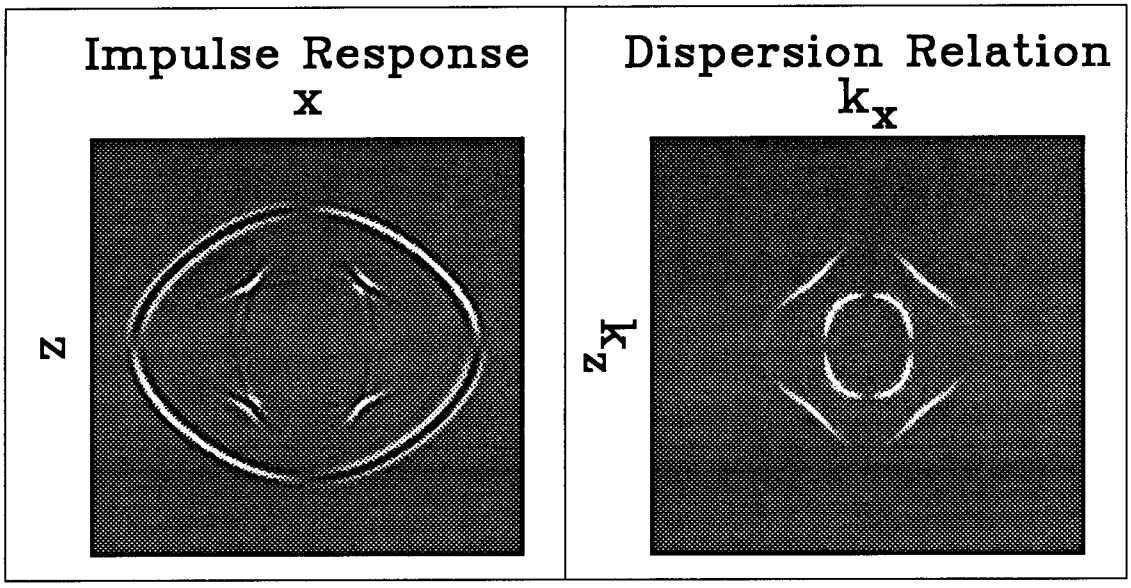

FIG. B.3. Left: A snapshot of an anisotropic wavefield. The model is "Greenhorn Shale" (Jones and Wang, 1981). The source is a vertical (Z) point force, and the X component of motion is shown. Right: The result of Fourier-transforming the aforementioned wavefield over x, z, and t; a "snapshot" at one ω of the complex absolute value of the X component is shown. The plot is just a dispersion relation calculated the brute-force way, by Fourier-transformation.

B.3 Symmetric properties of ellipses

In an isotropic medium, the group and phase-velocity curves are both circles. Since one over a constant is still a constant, the group and phase-slowness curves are also circular. If we perform a linear stretch on the coordinate axes, our isotropic medium becomes elliptically anisotropic, and our circular group-velocity curve becomes an ellipse. The similarity theorem of Fourier transforms tells us that if we stretch the x axis, say, then in the Fourier domain we have squeezed the k_x axis. This shows that our formerly circular dispersion relation in this case also becomes an ellipse. Thus, an elliptical group velocity goes with an elliptical phase slowness and vice-versa. (For a graphical example see the dashed thin curves in Figure B.4.)

While this property is easy to prove in this way, I know of no simple intuitive proof using the equations in Table B.1 directly (although tedious algebra will eventually show that the equations in Table B.1 do obey the stretch theorem as expected.)

These symmetric properties of ellipses prove important when considering the meaning of Normal Moveout (see sections 2.1.1 and 2.1.2).

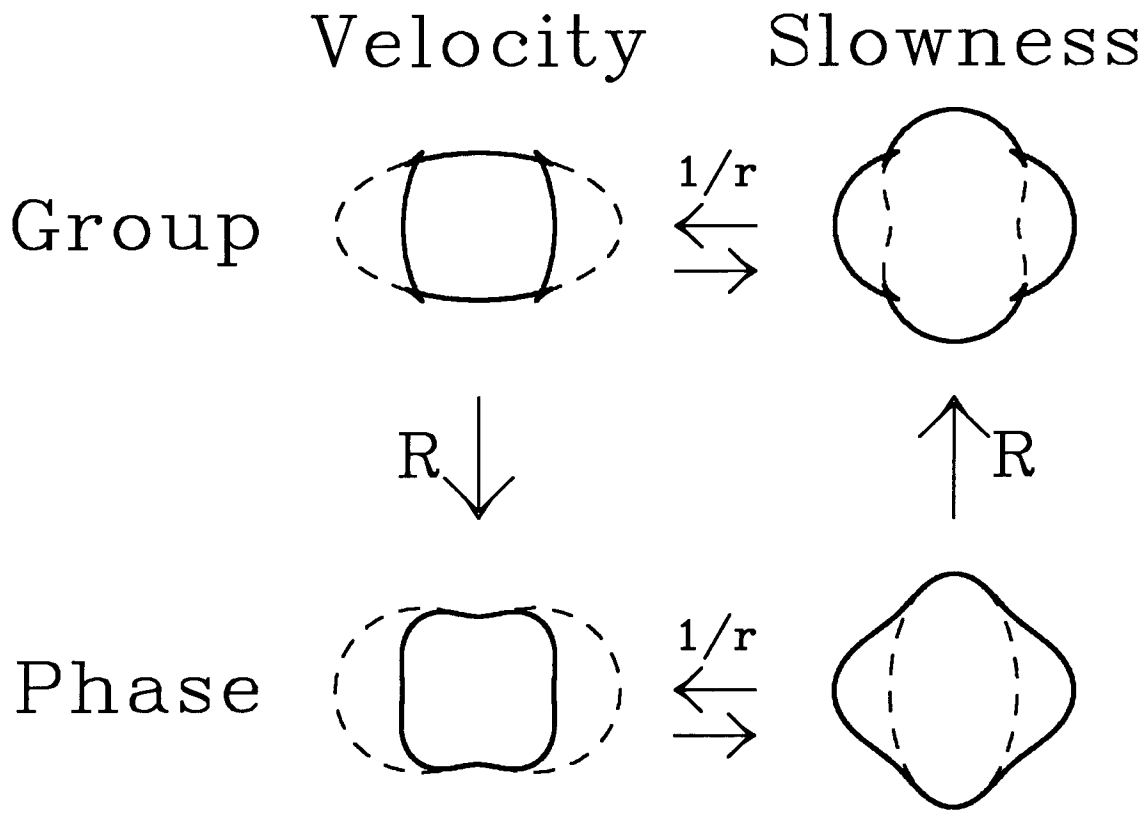

FIG. B.4. Group velocity (or impulse response), group slowness, phase velocity, and phase slowness (or dispersion relation) plots for the qSV mode of Greenhorn Shale (Jones and Wang, 1981) (thick solid line) and an elliptically anisotropic paraxial approximation to it (thin dashed line). The four plots are connected by two transformations, labeled "1/r" and "R" (defined in Table B.1). The transformation "1/r" is trivially its own inverse. More significantly, the combined transformation from the group-velocity curve (impulse response) to the phase-slowness curve (dispersion relation) "R $\circ$ 1/r" is also its own inverse. Compare the group velocity and phase slowness plots shown here with the ones in Figure B.3 calculated a completely different way.

B.4 Wavefront cusps (triplications)

Under what conditions can V_r become a multi-valued function of ϕ_r, resulting in cusps on the wavefront? (A good finite-difference model example is the qSV wavefront in Figure B.3.)

In section B.2 we noted that the group-direction vector is always perpendicular to the corresponding point on the phase-slowness curve. Thus if $\Lambda_w(\phi_w)$ is convex, ϕ_r increases as ϕ_w increases and V_r is a single-valued function of ϕ_r as well as ϕ_w, and there are no wavefront cusps. (In section A.2 we saw that $\Lambda_w(\phi_w)$ is single-valued.)

Cusps occur when ϕ_r instead of continuing forward as ϕ_w increases temporarily stops and goes backwards because $\Lambda_w(\phi_w)$ has a concavity. When this happens, the same value of ϕ_r is assumed for three different values of ϕ_w, and for this reason a cusp is also sometimes called a *triplication*. Mathematically, a cusp occurs whenever

$$\frac{d\phi_r}{d\phi_w} < 0. \tag{B.3}$$

(For an example of a cusp in three dimensions, see Figure 3.21.)

Starting from equation (B.2) and applying a bit of algebra involving multiplying through by guaranteed positive terms reduces equation (B.3) to:

$$\frac{d^2 V_w}{d\phi_w^2} < -V_w. \tag{B.4}$$

Although equation (B.4) seems innocent enough, the algebra it entails is usually quite horrendous in practice, even for relatively "simple" kinds of anisotropy. (For an example of using equation (B.3), see page 26.)

Appendix C

Parameters used in examples

C.1 Introduction

One goal of mine has been that any figure contained herein should be independently reproducable. I did not want to clutter up the text unnecessarily with lists of elastic constants, so all the elastic constants are given here instead, with some additional notes as to why I used those *particular* elastic constants. (More information helpful for reproducing my results can be found in the other sections of this appendix.)

C.2 Tables of 2D elastic constants

Table C.1 lists all the two-dimensional elastic constants used in the thesis.

Notes for Table C.1:

1. Isotropic.
2. 5000-foot depth Greenhorn Shale (Jones and Wang, 1981), my favorite anisotropic medium. (The original reference gives $C_{11} = 3.43$, not 3.41; I slipped a digit!)
3. "Black Shale", sample numbers 10931 and 10164 from the Bakken formation (Vernik and Nur, 1990).
4. Symmetry value of C_{13}, $C_{13} = -C_{55}$; borderline anomalously polarized.
5. Borderline triplication.

Figure	Name	Note #	C_{11}	C_{33}	C_{55}	C_{13}	C_{66} or ρ
2.4 #1, 2.7 bot		4, 7	3.41	2.27	.54	-.54	
2.4 #2, 2.7 mid, B.1, B.3, B.4	Greenhorn Shale	2, 7	3.41	2.27	.54	1.07	
2.4 #3, 2.20–2.22		5	3.41	2.27	.54	1.3698	$\rho = 2.42$
2.4 #5, 2.7 top, 2.18, 2.19		8	3.41	2.27	.54	1.68825	$\rho = 2.42$
2.4 #7		5	3.41	2.27	.54	1.88885	
2.4 #8, 2.8 top		5, 6	3.41	2.27	.54	2.01243	
2.4 #9, 2.8 mid		9, 6	3.41	2.27	.54	2.30965	$C_{66} = 1.06$
2.4 #10, 2.8 bot		10, 6	3.41	2.27	.54	2.78	
2.10 top		15, 7	3.41	2.27	.54	-2.15	
2.5 #1		4, 11, 7	3.41	3.41	.54	-.54	
2.5 #2		4, 7	3.41	2.00	.54	-.54	
2.5 #3		4, 7	3.41	.60	.54	-.54	
2.5 #4		4, 12, 8	3.41	.54	.54	-.54	
2.5 #5, 2.10 mid		4, 13, 8	3.41	.30	.54	-.54	
2.6 #1, 2.9 top		6	3.00	1.35	1.00	.50	
2.6 #2, 2.9 mid		13, 6	3.00	1.35	1.75	.50	
2.6 #3, 2.9 bot		13, 14, 6	3.00	1.35	3.50.	.50	
2.10 bot		16, 13, 14, 9	3.00	3.00	4.00	-2.73	$C_{66} = .5$
2.11–2.15	Bakken Shale #10931	3	5.12	2.71	1.01	1.74	$\rho = 2.36$
2.16, 2.17	Bakken Shale #10164	3	4.09	2.69	1.05	.85	$\rho = 2.30$
2.24 Iso, 2.25 lef	Isotropic	1	2.27	2.27	.54	1.19	$\rho = 1.$
2.24 Ani, 2.25 rig		7	3.41	2.27	.54	.30	$\rho = 1.$
2.26 lo lef	Greenhorn Shale	2, 7	3.41	2.27	.54	1.07	$\rho = 1.$
2.26 lo rig		17	2.88	2.27	1.35	-.49	$\rho = 1.$
4.8 top	Isotropic	1	1.	1.	.3	.4	
4.8 bot		5	1.	1.	.3	.23427	
4.9 top, 4.4		7	1.	3.	.3	.7	
4.9 bot		6	1.	1.	.3	.65	
4.10 Iso, 4.11 Iso	Isotropic	1	4.41	4.41	.81	2.79	$\rho = 1.$
4.10 Ani, 4.11 Ani		7	8.45	8.45	2.45	2.00	$\rho = 1.$

Table C.1. Elastic constants for two-dimensional media used in figures. When the density $\neq 1$ is given, it is in gm/cm^3, and the elastic constants are in units of 10^5 bars (i.e. 10^{11}gm/(s^{2}cm)). If no density is given or the density is 1 the units are arbitrary.

6. On-axis triplication.

7. Off-axis triplication.

8. At elliptic constraint.

9. Borderline energy conservation. (Note this depends on an assumed value of C_{66} which otherwise effects only the SH mode; the assumed value of C_{66} is given in parenthesis in the rightmost column.)

10. Borderline positive phase velocities.

11. $C_{33} = C_{11}$.

12. $C_{33} = C_{55}$; borderline anomalously polarized.

13. $C_{33} < C_{55}$; anomalously polarized.

14. $C_{11} < C_{55}$; anomalously polarized.

15. $C_{13} < -C_{55}$; anomalously polarized.

16. Group velocity nearly isotropic.

17. Shares Greenhorn Shale's particle motion behavior, but not particle motion direction.

C.3 Tables of 3D TI and orthorhombic elastic constants

Table C.2 lists all the three-dimensional transversely isotropic or orthorhombic elastic constants used in the thesis.

Notes for Table C.2 (the note number is in the column labeled "N"):

1. A "canonical" orthorhombic medium. Although the medium as a whole is strongly anisotropic, the P wave alone is isotropic. In each symmetry plane there are pure SH *and* SV modes, with one S mode circular and the other elliptical.

2. "Isotropic"; actually it is a transversely isotropic medium that is *almost* isotropic. The elastic constants are carefully chosen so the qSV and SH slowness surfaces do not intersect anywhere except at the mandatory kisses on the k_z axis. An additional

Figure	N	C_{11}	C_{22}	C_{33}	C_{44}	C_{55}	C_{66}	C_{23}	C_{13}	C_{12}
3.1, 3.2, 3.10, 3.11	1	1.02	1.01	1.03	.253	.301	.356	.501	.403	.302
3.3	2	1.	1.0001	.98	.290001	.29	.3	.42	.4201	.4
3.16 up lef	3	1.	.999	1.	.299	.301	.3	.4	.399	.401
3.6 rig	4	1.1	1.1	.3	.4	.4	.55	-.4	-.4	0.
3.14 top lef, 3.17, 3.21	5	341.	341.	227.	54.	54.	106.	107.	107.	129.
3.14 top rig	6	338.67	324.76	225.4	51.43	54.	100.95	101.91	105.07	122.86
3.8, 3.12, 3.13, 3.14 mid lef, 3.18–3.20, 3.22–3.27, 3.37	6	336.56	310.	223.95	49.09	54.	96.36	97.27	103.32	117.27
3.14 mid rig	7	320.74	308.08	222.46	49.09	51.43	92.17	95.58	98.46	111.76
3.14 bot lef	7	306.33	306.33	221.10	49.09	49.09	88.33	94.04	94.04	106.74
3.14 bot rig	7	281.08	303.26	218.72	49.09	45.	81.54	91.34	86.29	97.94
3.28–3.31, 3.38, 3.39	8	1.	1.	1.	.342705	.25	.45	.31459	.5	.1
3.32–3.36	9	1.1	1.1	.4	.3	.5	.4	-.4	-.4	.3

Table C.2. Elastic constants for orthorhombic and TI three-dimensional media used in figures.

slight perturbation breaks the perfect TI symmetry. This was necessary to keep the LINPACK (Dongarra, Moler, Bunch, and Stewart, 1979) singular value decomposition routine from exploding. (Why the LINPACK routine **dsvdc** should occasionally blow up when given a 3×3 matrix with two equal eigenvalues is another question, but it does!)

3. A "nearly isotropic" orthorhombic medium. The non-orthorhombic plots in Figures 3.16, 3.15, and 3.9 use perturbed versions of these elastic constants. The perturbation factor for all these plots is
   $C_{16} = .001$, $C_{56} = -.001$, $C_{34} = .001$, and $C_{25} = -.001$,
   with a multiplier of
   .5 for the upper right plot in Figure 3.16,
   .59 for the lower left plot in Figure 3.16,
   .75 for the lower right plot in Figure 3.16, and
   1. for Figures 3.9 and 3.15.

4. An anomalously polarized transversely isotropic medium. Since it is TI there is a pure SH mode, but the other two modes are neither qS nor qP.

5. Greenhorn Shale again (Jones and Wang, 1981). (Note the original reference lists $C_{11} = 343$, not 341; this difference is inconsequential.) The density is 2.42 gm/cm^3. The stiffness constants are given in units of kilobars (i.e. 10^9gm/(s^{2}cm)).

6. "Cracked Greenhorn Shale", constructed by taking the elastic constants for Greenhorn Shale and using Schoenberg-Muir theory (Schoenberg and Muir, 1989) to add cracks in the x-z plane (Nichols, Muir, and Schoenberg, 1989), resulting in an orthorhombically anisotropic medium. (In Dave Nichols' notation the x-z cracking is 5% and 10% for the two examples.) The density is unchanged by the cracking.

7. "Doubly Cracked Greenhorn Shale", constructed by adding another set of cracks (this time in the y-z plane) to "Cracked Greenhorn Shale". (In Dave Nichols' notation the y-z cracking is 5%, 10%, and 20% for the three examples, in addition to a constant 10% x-z cracking.) The density is unchanged by the cracking.

8. Another "canonical" medium like the one described in note 1, although less strongly anisotropic this time. The important property here is not the simple behavior in

the symmetry planes, but that there are four well-separated singularities of order +1. To get the medium actually used in the examples, the original "canonical" medium was rotated 43 degrees clockwise about the $+k_x$ axis so as to position one of the singularities almost exactly on the new k_z axis. The rotated medium (the one used in the examples) has elastic constants $C_{11} = 1.$, $C_{12} = 0.286049$, $C_{13} = 0.313951$, $C_{14} = 0.199513$, $C_{22} = 1.$, $C_{23} = 0.314590$, $C_{33} = 1.$, $C_{44} = 0.342705$, $C_{55} = 0.343024$, $C_{56} = -.0997564$, and $C_{66} = 0.356976$.

9. This is a simple "triply connected" orthorhombic medium. (All three wave surfaces are linked.) Musgrave (1981) gives spruce wood as a physically occurring example of such a medium. Another example is Tellurium Dioxide, a crystal famous in acousto-optics for its rather *extreme* anisotropy (Auld, 1973). I chose not to use either of these examples because they would have made for an overly complex figure. Both triplicate extremely strongly in addition to displaying anomalous polarizations and being triply connected.

As a final aside, the elastic constants for Figure 3.7 are $C_{11} = .75$, $C_{22} = .70$, $C_{33} = .80$, $C_{44} = 1.$, $C_{55} = 1.05$, $C_{66} = .3$, $C_{23} = -.5$, $C_{13} = -.5$, $C_{12} = .15$, and $C_{15} = .25$.

C.4 Latitude and longitude

Many figures are labeled according to the "longitude" of the slice. My convention is that the z (or k_z) axis defines the polar axis, with the x-y (or k_x-k_y plane) defining the equator. Longitude 0° is the $+x$-$+z$ plane, longitude 90° is the $+y$-$+z$ plane, longitude 180° is the $-x$-$+z$ plane, etc.

The latitude-longitude system can also be used to specify the projection viewpoints of the various three-dimensional plots in the thesis; this is done in Table C.3. (The stereo pairs are offset ±3° horizontally from the central values given in the table. All projections are from infinity.)

C.5 Modeling methods used

Three different finite-difference modeling programs were used, all written by John Etgen. The two-dimensional examples in section 2.4.1 were all calculated on a 256^2 grid using the program "`aelastic2dpsv`". (This program was also used for the examples in

Figure	Latitude	Longitude	West	East	South	North	Rotation
3.2, 3.10	27.5	59.2					
3.11	41.4	0.	-45.	45.	10.	75.	
3.3, 3.6, 3.9	30.5	31.2					
3.7	-20	-40	0.	1.	-67.5	50.	
3.15, 3.16	25.	65.	22.5	112.5	-22.5	67.5	
3.19	34.5	28.1					$-60°$ about z
3.21–3.25	30.5	25.1					$-60°$ about z
3.28, 3.29	23.5	21.2	90.	360.	51.	90.	
3.32	21.5	52.2					

Table C.3. Projection viewpoints for various 3D figures, in degrees North and East. Some of the figures show only a small Saskatchewan-shaped window of the surface; if this is the case, the bounding latitude and longitude limits are given in the next four columns. If a rotation was applied to the elastic constants before the plot was calculated, the angle and the axis are given in the last column. (Point your thumb out along the + axis to get the sign right.) Note the *plotted* axes are rotated with the medium, even though the viewpoint angle is specified in terms of the real unrotated ones.

section 2.5, but with larger grids.) **Aelastic2dpsv** is a straightforward staggered-grid high-order finite-difference in space second-order finite-difference in time modeling program incorporating absorbing boundaries and a free surface. (My examples never made use of the absorbing boundaries.) It allows standard two-dimensional transverse isotropy, with the x and z axes as symmetry lines.

The two-dimensional examples in section 2.4.2 were all calculated on a 243^2 grid using the program "**aelastic2dmapt_per**". This is a sophisticated pseudo-spectral finite-difference in space Chebychev-polynomial finite-difference in time modeling program incorporating mapped grids. (I did not use the mapped grids for my examples.) It uses centered derivatives calculated using odd-order FFT's. For my purposes its main advantage is that it allows arbitrary two-dimensional anisotropy. (I.e., it knows about C_{35} and C_{15}.)

The three-dimensional examples in Chapter 3 were calculated on a 128^3 grid using "**spectral3d**". This program is fully spectral over all three space coordinates, and so can only handle homogeneous media with periodic boundaries. It is a Chebychev-polynomial finite-difference method in time. The spectral derivatives allow the wavefield to be sampled very close to the spatial alias, which is a big advantage. It also allows a complete set of

21 elastic constants to be specified.

See Etgen and Dellinger (1989) for more details and references.

C.6 Miscellaneous comments about notation

C.6.1 P, SV, SH as directions

I often use {P, SV, SH} as a convenient coordinate system for specifying particle-motion directions. When used this way "P", for example, indicates the component of motion along a radial line out from the source, nothing more. Similarly, "SV" indicates S motion within a plane under consideration (such as the plane of the two-dimensional plot), while "SH" indicates S motion perpendicular to the plane.

C.6.2 {XYZ}{xyz} notation

Occasionally I use a notation like "Xz" when discussing source and receiver orientations. This is a notation invented by Corrigan (1987). The capital letter indicates the source orientation, the lower-case letter the receiver orientation. In the absence of an imposed global coordinate system, z means down, x means horizontal and along the source-receiver line, and y means horizontal and perpendicular to the source-receiver line.

Bibliography

Adams, D., 1982, Life, the universe, and everything: Pan Books Ltd

Aki, K., and Richards, P. G., 1980, Quantitative seismology, theory and methods, vol. 1: W. H. Freeman and Company

Alford, R. M., 1986, Shear data in the presence of azimuthal anisotropy: Dilley, Texas: Expanded abstracts of the SEG, **56**, 476–479.

Auld, B. A., 1973, Acoustic fields and waves in solids, vol. 1: John Wiley and Sons

Bachman, R. T., 1979, Acoustic anisotropy in marine sediments and sedimentary rocks: Journal of Geophysical Research, **84**, B13, 7661–7663.

Berry, M. V., 1990, Anticipations of the geometric phase: Physics Today, **43**, 12, 34–40.

Berry, M. V., and Hannay, J. H., 1977, Umbilic points on Gaussian random surfaces: Journal of Physics A, **10**, 11, 1809–1821.

Blair, J. M., and Korringa, J., 1987, Aberration-free image for SH reflection in transversely isotropic media: Geophysics, **52**, 1563–1565.

Booth, D. C., and Crampin, S., 1983, The anisotropy reflectivity technique: theory: Geophys. J. R. astr. Soc., **72**, 755-766.

Boothby, W. M., 1975, An introduction to differentiable manifolds and Riemannian geometry: Academic Press

Burridge, R., 1967, The singularity on the plane lids of the wave surface of elastic media with cubic symmetry: Quart. Journ. Mech. and Applied Math., **20**, 1, 41–56.

Chapman, C. H., and Shearer, P. M., 1989, Ray tracing in azimuthally anisotropic media—II. Quasi-shear wave coupling: Geophysical Journal, **96**, 65–83.

Claerbout, J.F., 1985, Imaging the Earth's interior: Blackwell Scientific Publication

Crampin, S., 1981, A review of wave motion in anisotropic and cracked elastic-media: Wave Motion, **3**, 343–391.

Crampin, S., and Kirkwood, S. C., 1981, Velocity variations in systems of anisotropic symmetry: J. Geophys., **49**, 35–42.

Crampin, S., and Yedlin, M., 1981, Shear-Wave Singularities of Wave Propagation in Anisotropic Media: Journal of Geophysics, **49**, 43–46.

Crandall, M. G., and Majda, A., 1980, Monotone difference approximations for scalar conservation laws: Mathematics of Computation, **34**, 149, 1–21.

de Klerk, J., and Musgrave, M. J. P., 1955, Internal conical refraction of transverse elastic waves in a cubic crystal: Proc. Phys. Soc. Lond. B, **68**, 2, 81–88.

Dellinger, J., 1989, Anisotropic travel-time inversion with error bars: theory: Stanford Exploration Project Report, **60**, 253–260.

Dellinger, J., and Etgen, J., 1990, Wave-field separation in two-dimensional anisotropic media: Geophysics, **55**, 914–919.

Dellinger, J., and Muir, F., 1988, Imaging reflections in elliptically anisotropic media: Geophysics, **53**, 1616–1618.

Dellinger, J., and Vernik, L., Do core-sample measurements record group or phase velocity?: in preparation

Devaney, A. J., and Oristaglio, L., 1986, A plane-wave decomposition for elastic wave fields applied to the separation of P-waves and S-waves in vector seismic data: Geophysics, **51**, 419–423.

Dongarra, J. J., Moler, C. B., Bunch, J. R., and Stewart, G. W., 1979, LINPACK User's guide: SIAM press

Engquist, B., and Osher, S., 1980, Stable and entropy satisfying approximations for transonic flow calculations: Mathematics of Computation, **34**, 149, 45–75.

Etgen, J., and Dellinger, J., Accurate wave-equation modeling: Expanded abstracts of the SEG, **59**, 494–497.

Federov, F. I., 1968, Theory of elastic waves in crystals: Plenum Press

Gajewski, D., and Pšenčík, I., 1987, Computation of high-frequency seismic wavefields in 3-D laterally inhomogeneous anisotropic media: Geophys. J. R. astr. Soc., **91**, 383–411.

Garmany, J., 1989, A student's garden of anisotropy: Ann. Rev. Earth Planet. Sci., **17**, 285–308.

Gilbert, F., and Dziewonski, A. M., 1975, An application of normal mode theory to the retrieval of structural parameters and source mechanisms from seismic spectra: Phil. Trans. R. Soc. Lond. A, **278**, 187–269.

Helbig, K., 1958, Elastische wellen in anisotropen medien, Teil I: Gerlands Beiträge zur Geophysik, **67**, 177–211.

Helbig, K., 1983, Elliptical anisotropy – Its significance and meaning: Geophysics, **48**, 825–832.

Helbig, K., 1984, Transverse isotropy in exploration seismics: Geophys. J. R. astr. Soc., **76**, 79–88.

Helbig, K., Foundations of anisotropy for exploration seismics: in preparation

Helbig, K., Rays and wavefront charts in gradient media: Geophysical Prospecting, **38**, 189–220.

Helbig, K., and Schoenberg, M., 1987, Anomalous polarization of elastic waves in transversely isotropic media: J. Acoust. Soc. Am., **81**, no. 5, 1235–1245.

Jech, J., and Pšenčík, I., 1989, First order perturbation method for anisotropic media: Geophysical Journal International, **99**, 369–376.

Jolly, R. N., 1956, Investigation of shear waves: Geophysics, **21**, 905–938.

Jones, E. A., and Wang, H. F., 1981, Ultrasonic velocities in Cretaceous shales from the Williston basin: Geophysics, **46**, 288–297.

Kawasaki, I., Mode-mode coupling of surface waves in an anisotropic medium: in preparation

Levin, F. K., 1978, The reflection, refraction, and diffraction of waves in media with an elliptical velocity dependence: Geophysics, **43**, 528–537.

Lyakhovitskiy, F. M., 1984, Transverse isotropy of thinly layered media: Geophys. J. R. astr. Soc., **76**, 71–77.

McGullagh, J., 1837, Geometrical proposition applied to the wave theory of light: Trans. Royal Irish Acad., **17**, 241–263.

McMechan, G. A., and Yedlin, M., J., 1981, Analysis of dispersive waves by wave field transformation: Geophysics, **46**, 869–874.

Meadows, M. A., 1985, The inverse problem of a transversely isotropic elastic medium: Ph.D. thesis, University of California, Berkeley

Mueller, M. C., 1990, Prediction of lateral variability in fracture intensity using multicomponent shear wave surface seismic as a precursor to horizontal drilling: Presented at the Fifth International Workshop on Seismic Anisotropy, Edinburgh, Scotland

Muir, F., Dellinger, J., Etgen, J. T., and Nichols, D., Modeling elastic fields across irregular boundaries: submitted to Geophysics

Muir, F., Dellinger, J., and Karrenbach, M., Elliptic approximations for TI media: in preparation

Musgrave, M. J. P., 1970, Crystal acoustics: Introduction to the study of elastic waves and vibrations in crystals: Holden-Day series in Mathematical Physics

Musgrave, M. J. P., 1981, On an elastodynamic classification of orthorhombic media: Proc. R. Soc. Lond. A., **374**, 401–429.

Nichols, D., Muir., F., and Schoenberg, M., 1989, Elastic properties of rocks with multiple sets of fractures: Expanded abstracts of the SEG, **59**, 471–474.

Nur, A., and Simmons, G., 1969, Stress-induced velocity anisotropy in rock: an experimental study: Jour. of Geophys. Res., **74**, 27, 6667–6674.

Postma, G. W., 1955, Wave propagation in a stratified medium: Geophysics **20**, 780–806.

Press, W. H., Flannery, B. P., Teukolsky, S. A., and Vetterling, W. T., 1988, Numerical Recipes in C, The Art of Scientific Computing: Cambridge University, 644-656.

Ray, J., 1670, English proverbs

Sakadi, Z., 1941, Elastic waves in crystals: Proc. Phys.–Math. Soc. Japan, **23**, 539–547.

Samec, P., 1991, Wave equation modeling: describing realistic media: Ph.D. thesis, Stanford University

Schoenberg, M., and Costa, J., The Insensitivity of Reflected SH Waves to Anisotropy in an Underlying Layered Medium: submitted to Geophysical Prospecting

Schoenberg, M., and Muir., F., 1989, A calculus for finely layered anisotropic media: Geophysics, **54**, 581–589.

Shearer, P., M., and Chapman, C., H., 1988, Ray tracing in anisotropic media with a linear gradient: Geophysical Journal, **94**, 575–580.

Sheriff, R. E., 1984, Encyclopedic dictionary of exploration geophysics: Society of Exploration Geophysicists

Strang, G., 1980, Linear algebra and its applications: Academic Press

Synge, J. L., 1957, Elastic waves in anisotropic media: J. Math. Phys., **35**, 323-334.

Uren, N. F., Gardner, G. H. F., and McDonald, J. A., 1990, Normal moveout in anisotropic media: Geophysics, **55**, 1634–1636.

Van Trier, J., and Symes, W., Upwind finite-difference calculation of traveltimes: Geophysics, **56**, in press.

Vernik, L., and Nur, A., Ultrasonic velocity and anisotropy of petroleum source rocks: The Bakken formation: Expanded abstracts of the SEG, **60**, 845–848.

Vidale, J., 1988, Finite-difference calculation of travel times: Bull. Seism. Soc. Am., **78**, 6, 2062–2076.

Willis, H. A., Rethford, G. L., and Bielanski, E., 1986, Azimuthal anisotropy: occurrence and effect on shear-wave data quality: Expanded abstracts of the SEG, **56**, 479–481.

Winsor, F., 1958, The space child's Mother Goose: Simon and Schuster

Winterstein, D. F., 1986, Anisotropy effects in P-wave and SH-wave stacking velocities contain information on lithology: Geophysics, **51**, 661-672.

Winterstein, D. F., 1990, Velocity anisotropy terminology for geophysicists: Geophysics, **55**, 1070-1088.

Woolf, H. B., 1975, Webster's new collegiate dictionary: G. & C. Merriam company

Author Index

(1981) Shear-wave singularities of wave propagation in anisotropic media, 5, 6, 75, 84, 94

Crandall and Majda

(1980) Monotone difference approximations for scalar conservation laws, 133

de Klerk and Musgrave

(1955) Internal conical refraction of transverse elastic waves in a cubic crystal, 102

Dellinger

(1989) Anisotropic travel-time inversion with error bars: theory, 47

Dellinger and Etgen

(1990) Wave-field separation in two-dimensional anisotropic media, 49

Dellinger and Muir

(1988) Imaging reflections in elliptically anisotropic media, 9

Dellinger and Vernik

(in preparation) Do core-sample measurements record group or phase velocity?, 37

Devaney and Oristaglio

(1986) A plane-wave decomposition for elastic wave fields, 60

Dongarra, Moler, Bunch, and Stewart

(1979) LINPACK user's guide, 169

Engquist and Osher

(1980) Stable and entropy satisfying approximations for transonic flow calculations, 127

Etgen and Dellinger

(1989) Accurate wave-equation modeling, 7, 119, 172

Federov

(1968) Theory of elastic waves in crystals, 5

Gajewski and Pšenčík

(1987) Computation of high-frequency seismic wavefields in 3-D laterally inhomogeneous anisotropic media, 7

Garmany

(1989) A student's garden of anisotropy, 7, 158

Gilbert and Dziewonski

(1975) An application of normal mode theory to the retrieval of structural parameters and source mechanisms from seismic spectra, 92

Helbig

(1958) Elastische wellen in anisotropen medien, 5

(1983) Elliptical anisotropy – Its significance and meaning, 5, 14

(1984) Transverse isotropy in exploration seismics, 3

(1990) Rays and wavefront charts in gradient media, 158

(in preparation) Foundations of anisotropy for exploration seismics, 25

Helbig and Schoenberg

(1987) Anomalous polarization of elastic waves in transversely isotropic media, 6, 22, 23, 37, 67

Jech and Pšenčík
(1989) First order perturbation method for anisotropic media, 77

Jolly
(1956) Investigation of shear waves, 2

Jones and Wang
(1981) Ultrasonic velocities in Cretaceous shales from the Williston basin, 2, 24, 31, 42, 58, 70, 82, 88, 95, 161, 162, 165, 169

Kawasaki
(in preparation) Mode-mode coupling of surface waves in an anisotropic medium, 93

Levin
(1978) The reflection, refraction, and diffraction of waves in media with an elliptical velocity dependence, 2, 5, 14

Lyakhovitskiy
(1984) Transverse isotropy of thinly layered media, 6, 28

McGullagh
(1837) Geometrical proposition applied to the wave theory of light, 4, 158

McMechan and Yedlin
(1981) Analysis of dispersive waves by wave field transformation, 159

Meadows
(1985) The inverse problem of a transversely isotropic elastic medium, 14

Mueller
(1990) Prediction of lateral variability in fracture intensity using multicomponent shear wave surface seismic as a precursor to horizontal drilling, 4

Muir, Dellinger, and Karrenbach
(in preparation) Elliptic approximations for TI media, 21

Muir, Dellinger, Etgen, and Nichols
(submitted) Modeling elastic fields across irregular boundaries, 140

Muir
(1989) pers. comm., 107
(1990) pers. comm., 150

Musgrave
(1970) Crystal acoustics, 5
(1981) On an elastodynamic classification of orthorhombic media, 6, 62, 170

Nichols, Muir, and Schoenberg
(1989) Elastic properties of rocks with multiple sets of fractures, 84, 169

Nur and Simmons
(1969) Stress-induced velocity anisotropy in rock: an experimental study, 2

Postma
(1955) Wave propagation in a stratified medium, 2, 158

Press et al.
(1988) Numerical Recipes in C, 121

Ray
(1670) English proverbs, v

Sakadi
(1941) Elastic waves in crystals, 29

Samec
(1991) Wave equation modeling: describing realistic media, 120

Schoenberg and Costa
(submitted) The insensitivity of reflected SH waves to anisotropy in an underlying layered medium, 6, 15

Schoenberg and Muir
(1989) A calculus for finely layered anisotropic media, 82, 169

Shearer and Chapman
(1988) Ray tracing in anisotropic media with a linear gradient, 47

Sheriff
(1984) Encyclopedic dictionary of exploration geophysics, 3

Strang
(1980) Linear algebra and its applications, 152

Synge
(1957) Elastic waves in anisotropic media, 5

Uren, Gardner, and McDonald
(1990) Normal moveout in anisotropic media, 47

Van Trier and Symes
(1991) Upwind finite-difference calculation of traveltimes, 7, 120, 126, 127, 132, 134

Vernik and Nur
(1990) Ultrasonic velocity and anisotropy of petroleum source rocks, 6, 37, 43, 165

Vidale
(1988) Finite-difference calculation of travel times, 120

Willis, Rethford and Bielanski
(1986) Azimuthal anisotropy: occurrence and effect on shear-wave data quality, 4

Winsor
(1958) The space child's Mother Goose, 119

Winterstein
(1986) Anisotropy effects in P-wave and SH-wave stacking velocities contain information on lithology, 3, 4, 45
(1990) Velocity anisotropy terminology for geophysicists, 17, 84

Woolf
(1975) Webster's new collegiate dictionary, 92

Index